



COMPARISON OF COMPUTATIONAL SCATTERING METHODS

THOMAS WRIEDT† and UTE COMBERG

Institut für Werkstofftechnik, Bremen, Germany

Abstract—There are various methods to compute electromagnetic scattering by arbitrarily shaped particles. The aim of this article is merely to give a short introduction to three very different types of methods and have a look at the applicabilities and shortcomings of each. At first some comments are made.

- to the Discrete Dipole Approximation (DDA), alias Coupled Dipole Method (CDM), as a special form of the Volume Integral Equation Method (VIE);
- to the Finite Difference Time Domain (FDTD) and
- to the Extended Boundary Condition Method (EBCM).

As an example the results and the parameters of different codes for a cube are compared to give just a hint of the computational demands. © 1998 Published by Elsevier Science Ltd. All rights reserved.

1. INTRODUCTION

We are interested in simulating optical particle size counters by performing light scattering computations. As it is not clear as to which scattering theory is best suited for application to this problem, we compare different ones concerning versatility, computational demand and accuracy of results.

As a test particle we chose a dielectric cube. This may be a single representation of crystals of an organic material.

Simulation of the light scattering process, governed by Maxwell's equations, is a non-trivial problem for irregular grains. As analytical techniques are restricted to some special cases, different numerical and semi-analytical methods are available to handle other geometries of scattering bodies. They may be divided into surface-based and volume-based methods, additionally into those methods derived from an integral and those based on a differential equation.¹

The methods were selected for particular reasons:

The Discrete Dipole Approximation (DDA) code DDSCAT by Flatau² is a public domain software, well worked out and stands therefore for the Volume Integral Equation (VIE) techniques, which are widely spread and have a lot of options to extend the theory.

The Finite Difference Time Domain (FDTD) code is also freely available, although it had to be modified for our purposes. This method is interesting, because it is conceptually simple and has in principle no restrictions whatsoever.

The Extended Boundary Condition Method (EBCM) finally, sometimes called T-Matrix Method, is very well known, the most analytical one and hopefully the least demanding in terms of computer memory.

Naturally, comparisons on different scattering methods have already been set up and published, but either they focus on just two methods,³ rotational symmetric bodies^{4,5} or variations of one method^{6,7} or they are held very general and do not contain many numerical examples.¹ In this paper each method will at first be introduced in short: DDA with an emphasis on the integral over the singularity, FDTD giving more practical hints and EBCM in a general basic view. Then a numerical example follows, including a table with computational demands and scattered intensity diagrams.

†To whom correspondence should be addressed.

2. VOLUME INTEGRAL METHODS

A standard practice to formulate the scattering problem is to derive a volume integral equation, which gives the field everywhere in terms of the incident and internal fields. This equation is then discretized, and the resulting method is called by several names proving its popularity: Method of Moments (MoM), Discrete Dipole Approximation (DDA), Coupled Dipole Method (CDM) or Volume Integral Equation Method (VIEM). Actually, there are not so many differences between the variants mentioned above. They all divide the scatterer into cells with constant internal field, often called dipoles, and use the point-matching technique to solve the field in these interacting cells. In DDA/CDM the role of dipoles as physical units is emphasized a bit more while the MoM/VIEM theory considers them just as an abstract mathematical tool. One actual difference seems to lie in the way evaluating the diagonal self-interaction term, called polarizability in the DDA-terminology. Thus we will have a closer look at this point.

The Discrete Dipole Approximation was first introduced by Purcell and Pennypacker⁸ in 1973. Since then many improvements of the theory have been made, including basic improvements⁹ of the accuracy as well as extensions for anisotropic scatterers and enhancement of the solving algorithms. A very important contribution was the use of a conjugate gradient algorithm combined with a Fast Fourier Transform to solve the equation system (e.g., for DDSCAT described in Ref. 10).

2.1. Integral equation

The basic formula of the Discrete Dipole Approximation is the Volume Integral Equation (VIE):

$$\mathbf{E}(\mathbf{r}) = \mathbf{E}_{\text{inc}}(\mathbf{r}) + k_0^2 \int_V \chi(\mathbf{r}') \mathbf{G}(\mathbf{r}, \mathbf{r}') \mathbf{E}(\mathbf{r}') d^3\mathbf{r}', \quad (1)$$

where $\mathbf{E}(\mathbf{r})$ represents the total, $\mathbf{E}_{\text{inc}}(\mathbf{r})$ the incident electrical field, $\chi = (\epsilon_r - 1)$ the susceptibility and k_0 the wavenumber of free space. An arbitrary point is denoted by \mathbf{r} , any point inside the Volume V of the scatterer by \mathbf{r}' , the scalar of the distance is given by $r = |\mathbf{r} - \mathbf{r}'|$ and its unit vector by $\mathbf{n} = \mathbf{r} - \mathbf{r}'/r$. $\mathbf{G}(\mathbf{r}, \mathbf{r}')$ is the Green's Dyadic for unbound, free space:

$$\begin{aligned} \mathbf{G}(\mathbf{r}, \mathbf{r}') &= \nabla \times \nabla \times \mathbf{G}(\mathbf{r}, \mathbf{r}') = \left[1 + \frac{1}{k_0^2} \nabla \nabla \right] \frac{1}{4\pi|\mathbf{r} - \mathbf{r}'|} e^{ik_0r - r'} \\ &= \left((\mathbf{1} - \mathbf{nn}) + \left(\frac{i}{k_0r} - \frac{1}{k_0^2 r^2} \right) (\mathbf{1} - 3\mathbf{nn}) \right) \frac{e^{ik_0r}}{4\pi r}. \end{aligned} \quad (2)$$

To get the CDM/DDA-formula one relates the polarization $\mathbf{P}(\mathbf{r})$ to the total electric field by $\mathbf{P}(\mathbf{r}) = \epsilon_0 \chi \mathbf{E}(\mathbf{r})$.

By using the same finite grid for integration (\mathbf{r}_j) and field discretization (\mathbf{r}_i) a system of equations in terms of the polarizations is obtained:

$$\mathbf{a}_{ii} \mathbf{P}(\mathbf{r}_i) = \mathbf{E}_{\text{inc}}(\mathbf{r}_i) - \sum_{j, j \neq i} \mathbf{a}_{ij} \mathbf{P}(\mathbf{r}_j). \quad (3)$$

Subsequently, the scattered far-field can be approximated as the one originating from a cloud of dipoles with the given polarizations.

2.2. Singularities

Special attention has to be paid in treating the singularity of the Green's function (in the \mathbf{a}_{ii} -terms in DDA), since inaccurate evaluation of the diagonal terms can lead to significant errors of the solution.

The classical procedure, excellently shown by Laktakhia and Mulholland⁷ and Peltoniemi¹¹ is to evaluate the integral employing the auxiliary function $\mathbf{G}_0(\mathbf{r}, \mathbf{r}') = \nabla \nabla (1/4\pi r)$, the long wave approximation $\mathbf{E}(\mathbf{r}) \approx \mathbf{E}(\mathbf{r}')$ and the Gauss-theorem as follows:

$$\int_{V_i} \mathbf{G}(\mathbf{r}, \mathbf{r}') \chi \mathbf{E}(\mathbf{r}') d^3\mathbf{r}' = \left(\int_{V_i} (\mathbf{G}(\mathbf{r}, \mathbf{r}') - \mathbf{G}_0(\mathbf{r}, \mathbf{r}')) \chi d^3\mathbf{r}' - \int_{\partial V_i} \frac{\mathbf{n}}{4\pi r^2} \chi d^2\mathbf{r}' \right) \mathbf{E}(\mathbf{r}). \quad (4)$$

As shown in Ref. 7 for a small sphere with the radius r_0 , the surface integral equals $-1/3$, and the volume integral becomes $(1 - \epsilon_r) 2/3[(1 - ik_0 r_0) e^{ik_0 r_0} - 1]$. This approximation is called the *strong form* of the MoM/CDM. Inserted into Eq. (3) it yields a polarizability α as follows:

$$\Rightarrow \alpha = 1/a_{ii} = \frac{\alpha_{CM}}{1 - \alpha_{CM}/\epsilon_0 2/3[(1 - ik_0 r_0) e^{ik_0 r_0} - 1]} \quad (5)$$

with α_{CM} being the Clausius–Mosotti polarizability. Still this derivation seems to be too bad an approximation to give satisfactory results. There are several approaches, trying to surpass this point:

- The so-called lattice correction technique by Draine and Goodman⁹ basically fits the polarizability in a way that a discrete [infinite?] grid looks continuous. The solution is called the Lattice Dispersion Relation, giving really good results for relative refractive indices up to $\Delta n \approx 2.5-3$.
- Another possible way to improve the self-term is to assume an electric field, that changes over the sub-volume V_i , as shown by Peltoniemi.¹¹ One more integral is considered, containing the difference $\mathbf{E}(\mathbf{r}) - \mathbf{E}(\mathbf{r}')$. Peltoniemi proposed a Taylor series expansion and managed the integral of the quadratic term of $\mathbf{E}(\mathbf{r}) - \mathbf{E}(\mathbf{r}')$. The polarizabilities gained by his results proved to be correct for relative refractive indices upto 4–5.
- And there is another idea, how to improve these integrals, developed recently by Piller.¹² The sampling of the electric field can be handled just as in signal processing employing sampling theory. That means the original field function can be reconstructed by weighting the discrete values with the SINC-function. This is equivalent to low pass-filtering in the frequency domain (the spectrum having been convoluted with a delta-series !) and may therefore be made with any filter function. And now we are at a tricky point: the SINC- or filter-function (actually the function of a Hamming-window was used by Piller) is not convoluted with the sampled electric field, but with the Green's function. By this, a new *filtered Green's function* is obtained analytically, having no singularities any more!

2.3 Efficient equation system solving/application range

The most important step to reduce the efforts spent in solving the equation system was the application of FFT techniques to the DDA. Since \mathbf{a}_{ij} depends only on the difference $|\mathbf{r} - \mathbf{r}'|$, the indices may be interchanged: $\mathbf{a}_{ij} = \mathbf{a}_{ji}$, which makes

$$\sum_j \mathbf{a}_{ij} \mathbf{X}_j = \mathbf{a} * \mathbf{X} \quad (6)$$

a convolution. So the sum is easily evaluated by 2 FFT-steps and one product. That means only $N * \log N$ additions instead of $N * N$.

Usually iterative solvers are used for the equation system. Here some efforts have been made, and an up to date QMR-solver is unbelievable fast compared to an old fashioned matrix inversion. This point is investigated further by Flatau [13] aiming for stable as well as fast convergence.

But there is still no really good way to evaluate the quality of the result other than comparing it to other methods. Especially for a refractive index $n > 2-3$ the classical CDM does not give useful results. It would be a big deal to find any self-contained error estimation for the volume integral methods analogous to the boundary conditions in the GMT (Generalized Multipole Technique).

The main limiting factor will be in most cases the computer capacities available. They set the absolute or just the sensible upper size of the particles to be handled by DDA. This size depends strongly on the shape and material of the particle as well as on the computer.

The parameter ranges, which must be kept strictly, are the limits of discretization and some material constraints:

$$k_0 \sqrt{\epsilon_r} \leq 0.5 \text{ as well as } \sqrt{\epsilon_r} < 2.5..3!!!! \text{ for the LDR-approximation}$$

$$\sqrt{\epsilon_r} < 5 \text{ for Peltoniemi's formula.}$$

3. FINITE DIFFERENCE TIME DOMAIN

Finite element and finite difference methods are primarily suited for bounded problems. Extending them to unbounded scattering problems requires truncation of the space to quite a small sub-volume around the scatterer and defining some debatable boundary conditions for the outer boundary. In addition one has to transform the near-fields to get the far-field scattering. Still they are straightforward, easy to understand and therefore often used for various electromagnetic calculations.

The Finite Difference Time Domain Method (FDTD) is the simplest way to solve the differential form of Maxwell's equations in the time domain. The scattered field formulation, employed in our code,¹⁴ seems to give more accurate results than the total field formulation.¹⁵ The differential equations:

$$\begin{aligned}\nabla \times \mathbf{E}^{i,s} &= \mu_i \frac{\mathbf{H}^{i,s}}{\partial t} - (\mu_i - \mu_0) \frac{\mathbf{H}_{\text{inc}}}{\partial t}, \\ \nabla \times \mathbf{H}^{i,s} &= \varepsilon_i \frac{\mathbf{E}^{i,s}}{\partial t} - (\varepsilon_i - \varepsilon_0) \frac{\mathbf{E}_{\text{inc}}}{\partial t} + \kappa_i \mathbf{E}^{i,s} - \kappa_i \mathbf{E}_{\text{inc}},\end{aligned}\tag{7}$$

are solved directly, being approximated by the difference equations:

$$\begin{aligned}\mu_i H_x^{i,s}(t + \Delta t) &= -\Delta t \left(\frac{E_y^{i,s}(z + \Delta z) - E_y^{i,s}(z)}{\Delta z} - \frac{E_z^{i,s}(y + \Delta y) - E_z^{i,s}(y)}{\Delta y} \right) + (\mu_i - \mu_0) \dot{H}_x^{\text{inc}} \\ &+ \mu_i H_x^{i,s}(t), \text{ etc.}\end{aligned}\tag{8}$$

The index i stands for a cell i of any material μ_i , ε_i and κ_i ; $\mathbf{H}^{i,s}$, $\mathbf{E}^{i,s}$ are the scattered and \mathbf{H}_{inc} , \mathbf{E}_{inc} are the incident fields. The magnetic field components are arranged half a cell size translated in the orthogonal coordinate directions (Yee-cell), so the algorithm is central. In the time domain method you have to time-step until a steady state solution is reached. This revealed to be the fact after approx. $N * 5$ steps for a N^3 -discretization points cubical space. At each time step either the electric or the magnetic fields are computed in turn, whereby they depend on the curls of the respectively other one and their own last time value.

This is an ideal scheme for parallel computing! As soon as such codes are available for scattering computations,^{15,16} the FDTD-method might win some more attraction for these applications.

The scatterer as well as about one wavelength space around it has to be discretized. This is necessary because the outer boundaries reflect parts of the waves. Special absorbing boundary conditions have to be elaborated to simulate the open boundaries required. This is one of the major problems of the FDTD, since it increases the computation volume eminently.

Another problem is the fixed step size, which forces the finest grid, which is needed at the places of shortest wave length only, on the entire space. But introducing different grid widths produces higher discretizational errors at the 'boundary' points, as can be seen by a Taylor series approximation.

At every point of the volume we had to use about 7 grid points per wavelength to get any useful result, about 10–15 gpts/ λ to get satisfactory and about 20 gpts/ λ to obtain good solutions ($\approx 5\%$).

Still the algorithm is easy to adapt to various problems and the method is capable to fulfill any differential equation, e.g. any material consistency and behavior, even anisotropy. In each computation cell you may introduce the equation, which shall be fitted. There are codes, which use higher order difference equations (e.g., the one developed by Cole¹⁷) hopefully gaining the same accuracy with lower grid point numbers, others, which include material boundary conditions, in order to better the behavior of the fields at these points.

Corresponding to the DDA method one problem occurs: one never knows how good the solution one obtained is, not even whether it is correct at all. This may be an advantage of the codes containing the boundary conditions!

Having gained the near-field, a far-field transformation has to be performed. We used the one, described by Taflove in Ref. 18. The near-fields are sampled on a surface ∂V enclosing the scatterer, Fourier-transformed and are replaced by currents. The scattering of these currents is properly

computed by taking them as sources in the well-known surface integrals:

$$\mathbf{E}_{\text{sca}} = \nabla \times \int_{\partial V} \mathbf{G}(\mathbf{r}, \mathbf{r}') \mathbf{J}_{\text{ma}}(\mathbf{r}') d^2 r' - \nabla \times \nabla \times \int_{\partial V} \frac{1}{ik_0} \mathbf{G}(\mathbf{r}, \mathbf{r}') \mathbf{J}_{\text{el}}(\mathbf{r}') d^2 r', \quad (9)$$

where $\mathbf{G}(\mathbf{r}, \mathbf{r}')$ is the Green's function of free space, $\mathbf{J}_{\text{el}}(\mathbf{r}') = \mathbf{n} \times \mathbf{H}(\mathbf{r}')|_{\partial V}$ the electric and $\mathbf{J}_{\text{ma}}(\mathbf{r}') = -\mathbf{n} \times \mathbf{E}(\mathbf{r}')|_{\partial V}$ the magnetic surface currents with \mathbf{n} being the surface normal and $\mathbf{H}(\mathbf{r}')|_{\partial V}$, $\mathbf{E}(\mathbf{r}')|_{\partial V}$ being the fields on this surface.

It is reasonable to approximate the far-fields by

$$\mathbf{E}_{\text{sca}} = \frac{1}{4\pi} \left(i\omega\mu_0 \left[\mathbf{1} - \frac{\mathbf{r}}{r^2} (\mathbf{r} \cdot \mathbf{A}) \right] - \frac{ik_0}{r} \mathbf{r} \times \mathbf{F} \right) \quad (10)$$

with

$$\mathbf{A} = \frac{e^{-ik_0 r}}{r} \int_{\partial V} e^{ik_0(\mathbf{r}\mathbf{r}'/r)} \mathbf{J}_{\text{el}}(\mathbf{r}') d^2 r'; \quad \mathbf{F} = \frac{e^{-ik_0 r}}{r} \int_{\partial V} e^{ik_0(\mathbf{r}\mathbf{r}'/r)} \mathbf{J}_{\text{ma}}(\mathbf{r}') d^2 r' \quad (11)$$

The results proved to be best, when the fields were sampled 6–8 cells away from the surface.

4. SURFACE INTEGRAL METHODS

An effective technique for analyzing the scattered field from an object was proposed by Waterman.^{19, 20} This approach is known as the Extended Boundary Condition Method (EBCM). In the EBCM one replaces the scattering object by a set of surface currents over the surface of the particle, so that in the exterior region the sources and fields are exactly the same as those existing in the original scattering problem. For surface current determination one uses the null-field condition for the total electric field within. The fields are expanded using a system of basis functions yielding for linear equation systems for the coefficients. The elements of this matrix are obtained by numerical integration. It is this point which grows computational extensive for irregular grains.

We note here, that in the case of tips or edges on the main surface, the fields should have singularities near the points of geometrical singularities. The usual technique is to smooth the geometrical singularities with certain radii of curvature, or to incorporate surface current densities capable of representing the correct singularity in sub-domains of interest. In the standard EBCM a simple technique which consists of the computation of the surface integrals by using Gaussian quadrature is often used.²¹ For particles consisting of more than one section one defines quadrature sample points and weighting values over each section separately, since Gaussian quadrature will not select the end points of integration.²² Formally, this technique is equivalent to the procedure of smoothing the geometrical singularities.

A different way to contribute to geometrical singularities is chosen for the EBCM with discrete sources (DS-EBCM). These sources are distributed depending on the actual form of the surface, resulting in distributed singularities of the sources, which may therefore be adapting to the fields better.

4.1. Standard EBCM

Let us consider a homogeneous dielectric object with the surface ∂V and the interior V_i . An arbitrary point is denoted by the position vector \mathbf{r} , while a point on ∂V is given by \mathbf{r}' . $k_i = k_0 \sqrt{\epsilon_i \mu_i}$ is the wave number in V_i .

In the view of the EBCM one replaces the scattering object by a set of surface currents \mathbf{e} and \mathbf{h} over the surface ∂V . The interior region of the scatterer has zero field by means of the equivalence theorem of surface currents. In addition the following equation is valid and useful once more:

$$\mathbf{E}(\mathbf{r}) = \mathbf{E}_{\text{inc}}(\mathbf{r}) + \nabla \times \int_{\partial V} \mathbf{G}(k_0|\mathbf{r} - \mathbf{r}') \mathbf{e}(\mathbf{r}') d^2 r' - \nabla \times \nabla \times \int_{\partial V} \frac{1}{ik_0} \mathbf{G}(k_0|\mathbf{r} - \mathbf{r}') \mathbf{h}(\mathbf{r}') d^2 r', \quad (12)$$

where $\mathbf{E}_{\text{inc}}(\mathbf{r})$ is the electric field of the incident wave and $\mathbf{G}(k_0|\mathbf{r} - \mathbf{r}')$ is the Green's function of unbounded space. For surface current determination one uses the null-field condition for the total electric field within ∂V . Therefore, the total electric field is expanded within an inscribed sphere

$\partial V_R \in V_i$ as

$$\mathbf{E}(\mathbf{r}) = \sum_{m \in \mathbb{Z}} \sum_{n > \max(1, |m|)} a_{mn} \cdot \mathbf{M}_{mn}^1(k_0 \mathbf{r}) + b_{mn} \cdot \mathbf{N}_{mn}^1(k_0 \mathbf{r}), \quad \mathbf{r} \in \partial V_R \in V_i, \quad (13)$$

where the expansion coefficients a_{mn} and b_{mn} are surface integrals depending on \mathbf{e} and \mathbf{h} , i.e.

$$\begin{aligned} a_{mn}(\mathbf{e}, \mathbf{h}) &= \frac{ik_0^2}{\pi} \int_{\partial V} [\mathbf{e}(\mathbf{r}') \cdot \mathbf{N}_{-mn}^3(k_0 \mathbf{r}') + i\mathbf{h}(\mathbf{r}') \cdot \mathbf{M}_{-mn}^3(k_0 \mathbf{r}')] d^2 r', \\ b_{mn}(\mathbf{e}, \mathbf{h}) &= \frac{ik_0^2}{\pi} \int_{\partial V} [\mathbf{e}(\mathbf{r}') \cdot \mathbf{M}_{-mn}^3(k_0 \mathbf{r}') + i\mathbf{h}(\mathbf{r}') \cdot \mathbf{N}_{-mn}^3(k_0 \mathbf{r}')] d^2 r'. \end{aligned} \quad (14)$$

Due to analytic continuation the null-field condition within V_i is equivalent to the condition that the coefficients a_{mn} and b_{mn} vanish.

A quasi-solution of the scattering problem can be obtained by approximating the surface currents in the mean square norm by the complete set of tangential *SVWF* (Spherical Vector Wave Functions) of the internal problem:

$$\begin{aligned} \begin{pmatrix} \mathbf{e}_{\hat{N}} \\ \mathbf{h}_{\hat{N}} \end{pmatrix} &\approx \left\{ \begin{pmatrix} \mathbf{n} \times \mathbf{M}_{mn}^1(k_i \mathbf{r}') \\ -i \sqrt{\frac{\epsilon_i}{\mu_i}} (\mathbf{n} \times \mathbf{N}_{mn}^1(k_i \mathbf{r}')) \end{pmatrix}, \begin{pmatrix} \mathbf{n} \times \mathbf{N}_{mn}^1(k_i \mathbf{r}') \\ -i \sqrt{\frac{\epsilon_i}{\mu_i}} (\mathbf{n} \times \mathbf{M}_{mn}^1(k_i \mathbf{r}')) \end{pmatrix} \right\} \\ &\text{with } m = -M, M; n \geq \max(1, |m|), N \end{aligned} \quad (15)$$

and by considering the truncated set of integral equations

$$\begin{aligned} a_{mn}(\mathbf{e}_{\hat{N}}, \mathbf{h}_{\hat{N}}) &= 0, \\ b_{mn}(\mathbf{e}_{\hat{N}}, \mathbf{h}_{\hat{N}}) &= 0, \quad m = -M, M, n \geq \max(1, |m|), N, \end{aligned} \quad (16)$$

where \hat{N} is a complex index incorporating M and N and \mathbf{n} is the outward unit normal to ∂V . This scheme allows us to obtain the amplitudes of the surface currents as solutions of a square linear system of equations.

Knowing the currents, Eq. (12) leads to the far-fields wanted.

4.2. EBCM with discrete sources

One of the great merits of the EBCM with discrete sources (DS) consists in the possibility of computing the scattering characteristics of particles with complex geometries for which the standard EBCM fails.²³ The explanation lies in the fact that distributed sources are better suited to model ‘difficult’ boundaries than localized sources. Various formulations of the EBCM can be constructed using DS located on auxiliary supports. As DS we used the system of magnetic and electric dipoles, the system of ‘Mie-potentials’ and the system of the lowest-order multipoles.²³ The strategy followed in these methods is to derive a set of integral equations for the surface current densities for various DS, and to approximate these densities by fields of DS.

Furtheron we restrict our analysis to the system of magnetic and electric dipoles

$$\mathbf{v}_t(\mathbf{r}, \mathbf{r}_p, \hat{\mathbf{r}}) = \frac{1}{k_t^2} (\hat{\mathbf{r}} \times \nabla \mathbf{G}(k_t | \mathbf{r} - \mathbf{r}' |)), \quad \mathbf{w}_t(\mathbf{r}, \mathbf{r}_p, \hat{\mathbf{r}}) = \frac{1}{k_t} (\nabla \times \mathbf{v}_t(\mathbf{r}, \mathbf{r}_p, \hat{\mathbf{r}})), \quad t = 0, i \quad (17)$$

Here $\hat{\mathbf{r}}$ is an arbitrary unit vector and \mathbf{r}_p is the source location. Let ∂V^- be the boundary of a finite region enclosed in V_i , and ∂V^+ be the boundary of a finite region enclosing V_i . We assume that the surfaces ∂V^- and ∂V^+ are smooth. The sequences of sources $\{\mathbf{r}_q\}_{q \in \mathbb{N}}$ and $\{\mathbf{r}_p\}_{p \in \mathbb{N}}$ are densely distributed on ∂V^- and ∂V^+ , respectively. At each point $\mathbf{r}_q \in \partial V^-$ and $\mathbf{r}_p \in \partial V^+$ we consider two tangential, linear independent unit vectors $(\hat{\mathbf{r}}_q^1, \hat{\mathbf{r}}_q^2)$ or $(\hat{\mathbf{r}}_p^1, \hat{\mathbf{r}}_p^2)$. Generally, the spectrum of eigenvalues of the interior region is $k^2(V_i)$. If $k_i^2 \notin k^2(V_i)$, then a quasi-solution of the scattering problem can be obtained by approximating the surface currents in the mean square norm by the complete set of

tangential components of the electric dipoles, i.e.

$$\begin{pmatrix} \mathbf{e}_N \\ \mathbf{h}_N \end{pmatrix} \approx \left\{ \left(\begin{array}{c} \mathbf{n} \times \mathbf{w}_p^1(k_i \mathbf{r}', \hat{\mathbf{r}}_p^1) \\ -i \sqrt{\frac{\epsilon_i}{\mu_i}} (\mathbf{n} \times \mathbf{v}_p(k_i \mathbf{r}', \hat{\mathbf{r}}_p^1)) \end{array} \right), \left(\begin{array}{c} \mathbf{n} \times \mathbf{w}_p(k_i \mathbf{r}', \hat{\mathbf{r}}_p^2) \\ -i \sqrt{\frac{\epsilon_i}{\mu_i}} (\mathbf{n} \times \mathbf{v}_p(k_i \mathbf{r}', \hat{\mathbf{r}}_p^2)) \end{array} \right) \right\}_{p=1, N} \quad (18)$$

and by considering the truncated set of integral equations

$$\int_{\partial V} [(\mathbf{e} - \mathbf{e}_0) \cdot \mathbf{v}_q(k_0 \mathbf{r}', \hat{\mathbf{r}}_q^1) + i(\mathbf{h} - \mathbf{h}_0) \cdot \mathbf{w}_q(k_0 \mathbf{r}', \hat{\mathbf{r}}_q^1)] d^2 \mathbf{r}' = 0 \quad (19)$$

$$\int_{\partial V} [(\mathbf{e} - \mathbf{e}_0) \cdot \mathbf{v}_q(k_0 \mathbf{r}', \hat{\mathbf{r}}_q^2) + i(\mathbf{h} - \mathbf{h}_0) \cdot \mathbf{w}_q(k_0 \mathbf{r}', \hat{\mathbf{r}}_q^2)] d^2 \mathbf{r}' = 0, \quad q = 1, N,$$

where we assume $k_0^2 \notin k^2(V_i^-)$.

Having gained the surface currents it is just one step to get the far-field scattering. As in standard EBCM the evaluation of the integrals is the computer time consuming part of the scheme.

5. NUMERICAL EXAMPLE

To get an idea of the computational efforts, the memory requirements as well as the CPU-time needed for simulating the scattering solutions of a cube obtained by some exemplary codes are compared.

The DDA-code DDSCAT,[†] version 5, by Draine and Flatau² is a public domain software. The VIE code, JSCAT,[‡] is programmed by Peltoniemi.¹¹ The FDTD program employs the code of Kunz and Luebbers¹⁴ and a simple far-field transformation. The EBCM-programs are nice codes by A. Doicu.²³

We took a cube as an example for a scatterer having edges. The refractive index was chosen to be $n = 1.5 + i0.0$, in order to have manageable storage demands for bodies of a few wave lengths' size. As results we present diagrams of the scattered intensities as well as of the corresponding relative differences. The table lists the required storage, the CPU-time and an "rms-error" as scale for the accuracy.

Figures 1–3 show the scattering diagrams for a cube of the side length a with $4a/\lambda = 3$ of VIE, DDA and EBCM, as well as the relative differences.

Figures 4–7 show the solutions for a cube of the side length a with $4a/\lambda = 5$ of FDTD resp. DDA in comparison to the EBCM-solution. Figures 8 and 9 are the results of the DS-EBCM. The relative errors are taken in comparison to the EBCM-results being the one, that is almost the "final"

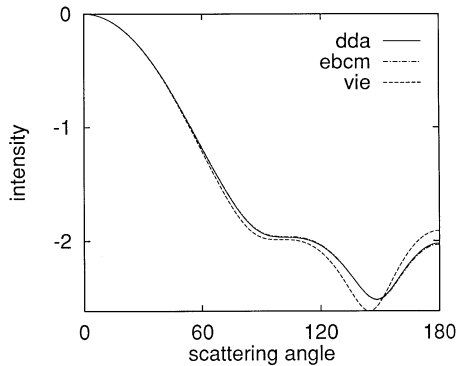


Fig. 1. Scattering diagram, obtained by DDSCAT with 125 000 dipoles, JSCAT using 216 cells and EBCM 112 functions, for a cube, $4a/\lambda = 3$, refractive index $n = 1.5 + i0.0$.

[†] <ftp://astro.princeton.edu/draine>.

[‡] <http://neutrino.pc.helsinki.fi/jouni/>.

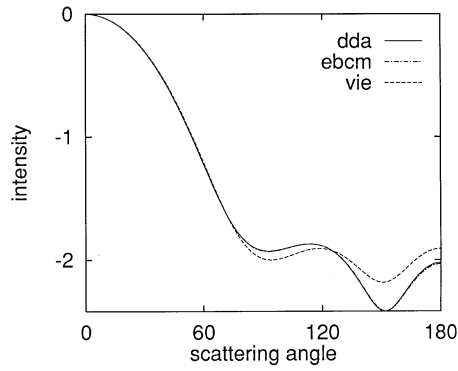


Fig. 2. Scattering diagram, obtained by DDSCAT with 125 000 dipoles, JSCAT using 216 cells and EBCM 112 functions, for a cube, $4a/\lambda = 3$, refractive index $n = 1.5 + i0.0$.

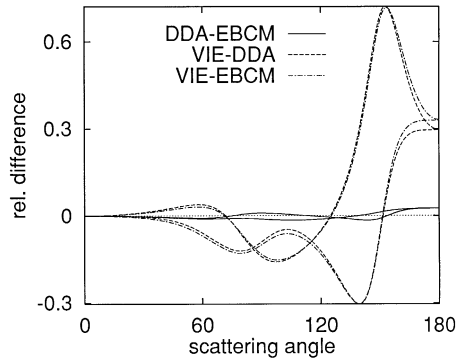


Fig. 3. Relative differences of DDSCAT and JSCAT, DDSCAT and EBCM, JSCAT and EBCM for a cube, $4a/\lambda = 3$, refractive index $n = 1.5 + i0.0$.

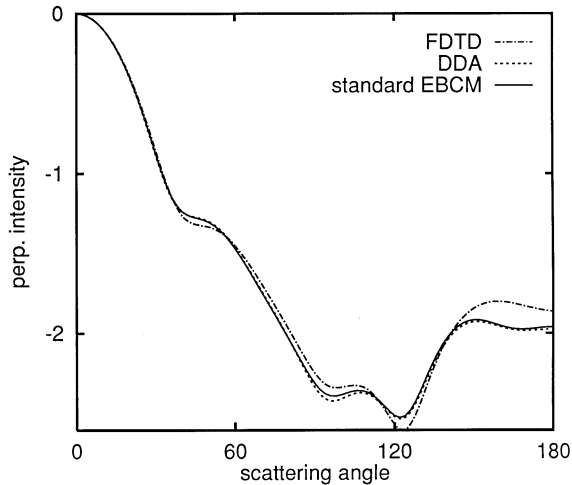


Fig. 4. Scattering diagram, obtained by DDSCAT with 216 000 dipoles, FDTD in a 512 000 points space and EBCM 104 functions, for a cube, $4a/\lambda = 5$, refractive index $n = 1.5 + i0.0$.

solution, where EBCM and DDA converge to. A cube of side length a with $4a/\lambda = 10$ is the scatterer of Figs. 10 and 11.

The results in the tables were achieved with the following parameters:

The FDTD80-space was $80 \times 80 \times 80$ cells big and 400 time steps were accomplished, the FDTD100 consisted of 100^3 cells and therefore 500 time steps taken etc. Of these cells 18^3 , 24^3 or 30^3

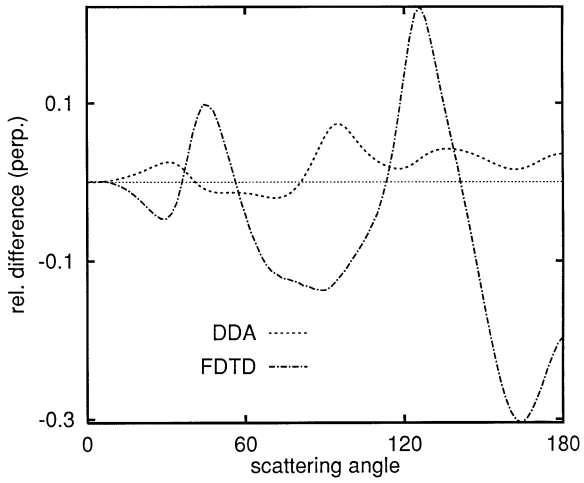


Fig. 5. Relative differences of the perpendicular intensity for DDSCAT and FDTD compared to EBCM results. The scatterer: a cube, $4a/\lambda = 5$, refractive index $n = 1.5 + i0.0$.

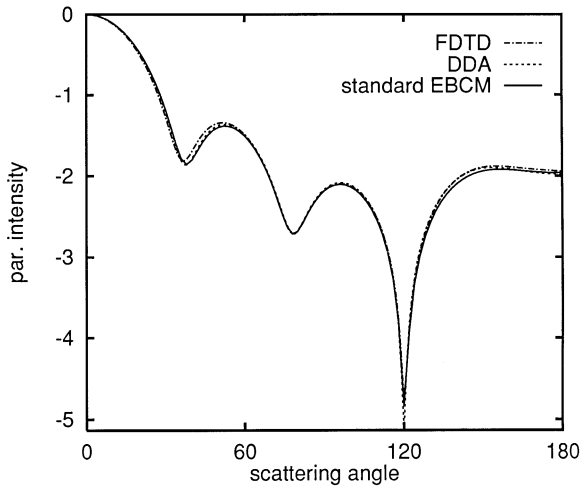


Fig. 6. The parallel scattered intensity analogous to Fig. 4. The scatterer: a cube, $4a/\lambda = 5$, refractive index $n = 1.5 + i0.0$.

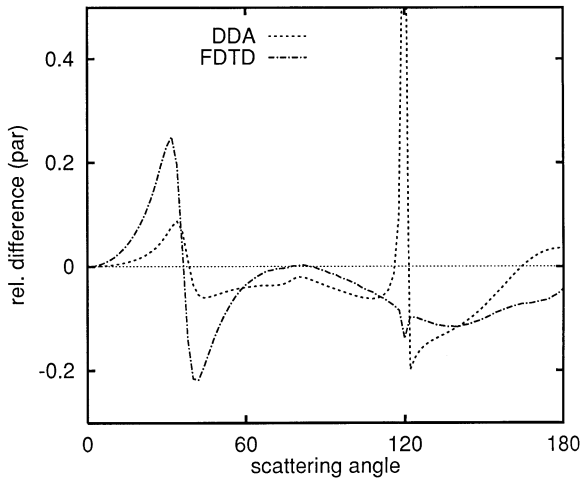


Fig. 7. Relative differences of the parallel intensity of Fig. 6. The scatterer: a cube, $4a/\lambda = 5$, refractive index $n = 1.5 + i0.0$.

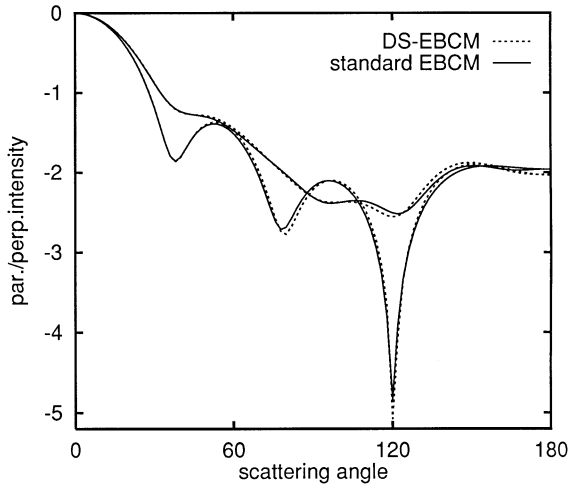


Fig. 8. Scattered Intensities computed by EBCM and DS-EBCM. The scatterer: a cube, $4a/\lambda = 5$, refractive index $n = 1.5 + i0.0$.

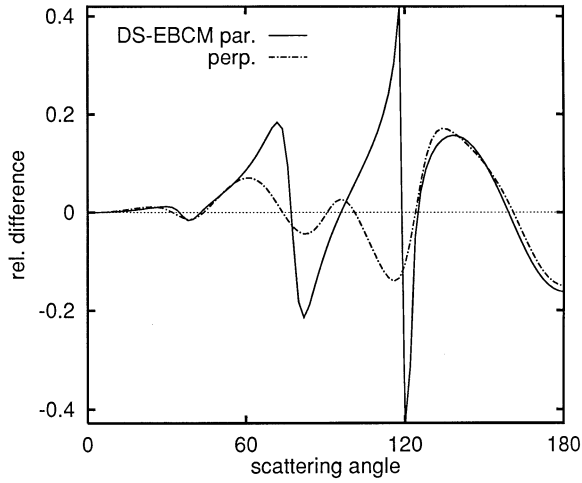


Fig. 9. Relative differences of Fig. 8, the DS-EBCM. The scatterer: a cube, $4a/\lambda = 5$, refractive index $n = 1.5 + i0.0$.

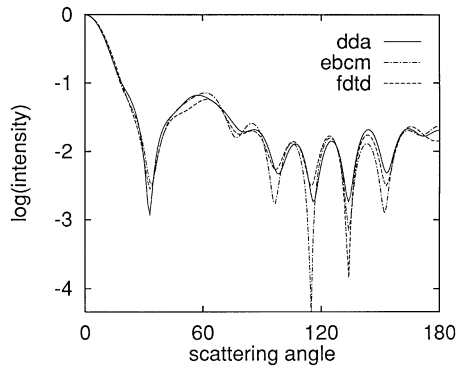


Fig. 10. Perpendicular scattered intensity of a cube, $4a/\lambda = 10$, refractive index $n = 1.5 + i0.0$. The FDTD space was 120^3 points, DDSCAT used 60^3 dipoles, EBCM $22^2 \times 6$ integration pts.

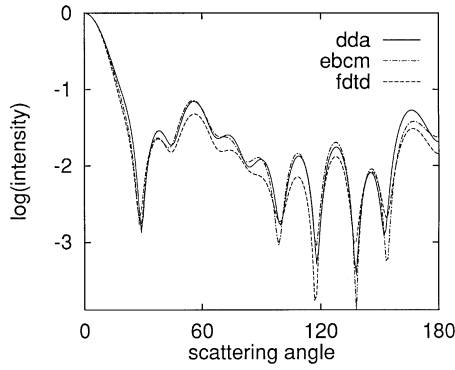


Fig. 11. Parallel scattered intensity of a cube, $4a/\lambda = 10$, refractive index $n = 1.5 + i0.0$.

Table 1. Data of simulations for three differently sized cubes of material $n = 1.334 + 0.0i$

Program	Storage (kB)	CPU-Time (s)	Errors (rms)		Disc. ($1/\lambda$)
<i>Cube $x = 3.0$</i>					
JSCAT	8100	789	0.11	0.10	10.0
JSCAT	18 100	1830	0.07	0.06	12.0
EBCM	1100	360	0.002	0.001	16.0
DDSCAT40	19 000	198	0.002	0.001	40.0
DDSCAT30	8504	59	0.002	0.001	30.0
<i>Cube $x = 5.0$</i>					
JSCAT	48 000	6800	0.10	0.08	7.2
FDTD80	16 320	350	0.15	0.08	10.8
FDTD100	32 000	715	0.10	0.08	14.4
DDSCAT54	37 710	540	0.003	0.003	32.4
DDSCAT40	18 170	320	0.002	0.002	24.0
DDSCAT30	8504	390	0.004	0.005	18.0
EBCM	1300	700	0.003	0.003	10.8
<i>Cube $x = 10.0$</i>					
EBCM	1550	1900	0.09	0.07	7.8
FDTD	53 344	760	0.13	0.23	13.1
DDSCAT50	37 710	1100	0.01	0.01	15.0
DDSCAT40	18 170	670	0.03	0.01	12.0

cells discretized the scatterer and, e.g., $41 \times 41 \times 6$ surface points were used for the far-field transformation. Ergo the discretization was 10–17, gpts/ λ .

DDSCAT50 utilized 50^3 dipoles to simulate the cube, DDSCAT45 45^3 , etc. This implies an discretization of 12–40 dipoles/ λ .

For the DS-EBCM-result 144 expansion functions were used and $16 \times 16 \times 6$ integration points taken, which means a discretization of 12.8 int.pts/ λ and 9.6 dipoles/ λ . For the EBCM-result (standard) 84–120 expansion functions were employed and $16 \times 16 \times 6$ to $20 \times 20 \times 6$ integration points taken, which means a discretization of 12.8 int.pts/ λ .

The rms-errors are normalized on the forward scattering intensity. They represent the rms-difference to the limiting values of DDA and EBCM, which differ in the order of 10^{-3} in most cases, a bit more for the big cubes.

Table 1 lists the output for scatterers of the material $n = 1.334 + 0.0i$, whereas Table 2 shows mostly the same “experiments” for a refractive index of $n = 1.5 + 0.0i$. The CPU-Time is taken on an IBM RISC/6000-595-workstation.

Figure 3 illustrates the excellent fitting of the DDA and the EBCM-results with a maximum difference of 5%, if the DDA dipole spacing is small and the EBCM solution is taken carefully. In this case the VIE-result seems to be the one with the lowest accuracy.

Table 2. Data of simulations for three differently sized cubes of material $n = 1.5 + 0.0i$

Program	Storage (kB)	CPU-Time (s)	Errors (rms)		Disc.
<i>Cube $x = 3.0$</i>					
JSCAT	48 100	1850	0.07	0.10	10.7
EBCM	1100	350	0.002	0.001	14.2
DDSCAT40	19 000	200	0.001	0.001	35.6
DDSCAT30	8500	67	0.001	0.001	26.7
<i>Cube $x = 5.0$</i>					
JSCAT	48 000	6800	2.00	2.00	6.4
FDTD120	53 500	750	0.06	0.15	12.8
DDSCAT60	48 500	1250	0.01	0.01	32.0
DDSCAT40	18 000	290	0.01	0.01	21.3
EBCM	1500	1080	0.01	0.03	10.6
DS-EBCM	1728	1600	0.06	0.03	8.5
<i>Cube $x = 10.0$</i>					
EBCM	2000	2100	0.23	0.13	9.6
FDTD120	53 500	750	0.13	0.23	10.7
DDSCAT50	37 500	1100	0.01	0.01	13.3
DDSCAT40	18 000	650	0.06	0.05	10.7

Figures 4–7 show roughly the same habitude for the cube with $4a/\lambda = 5$ of FDTD resp. DDA in comparison to the EBCM-solution. The DDA-curves agree well with the EBCM-results, FDTD differs mainly in the backscattering direction for one polarization. Since the (angular) relative differences are shown and the scale is logarithmic, naturally the lower points of the curves have still “high” differences. Figure 9 showing the difference of the DS-EBCM and the EBCM-results, illustrates that some discrepancies are remaining, which should decrease, if higher order poles are taken into account.

A cube of side length a with $4a/\lambda = 10$ is the scatterer of Figs. 10 and 11. This case is deviant to all former ones, because we reached the limits of our computer. Although quite a rough discretization is taken, the *qualitative* form of the diagrams, the minimum locations, etc. are still very similar for the methods.

The comparison for the two different materials show how sensitive the methods are to the refractive index, the discretization per wavelength.

6. CONCLUSION

The FDTD method is very memory consuming, which is mainly caused by the huge volume that has to be discretized in case of a dielectric scatterer. This is probably the cause for the remaining differences to the DDA and EBCM results for our scatterers: the number of cells for FDTD was not big enough to reach high accuracy, where the size of the particle did not affect the grid width very much, since most cells of the computational volume belonged to the surrounding space. But even with these restrictions quite good and reliable approximations can be obtained. Finite differences need a lot of CPU-time, since each orientation of a particle has to be evaluated separately. The main advantage is, that it is really simple and general in its formulation. The probability to make a basic error is very low if the gridding is just fine and the space around the particle big enough. Very complex material data may be considered easily, various difference equations be defined for even specific parts of the computational space.

The DDA/CDM methods are reasonably fast, but still memory consuming. Well worked-out codes exist for scattering applications. The DDA-code DDSCAT for example is easy to apply to various geometries and material configurations, a number of different solvers is implemented already. And the solutions show a steady convergence over the dipole number for our cubes.

Slower and the most memory demanding of all, but more general are VIE codes like JSCAT, planned for including anisotropy. No symmetry of the matrix is assumed.

As expected the EBCMs are the best suited for our problem, requiring *very little memory* and affordable CPU-time. At this point one should consider, that with this method, orientational

averages are gained almost for free. Still one has to keep in mind, that the solutions have to be investigated for convergence, since they tend to oscillate. Each new geometry has to be observed carefully. In the standard EBCM the surface has to be divided into sub-surfaces for integration for each scatterer newly depending on the tips and edges of its surface. The DS-EBCM requires a choice of appropriate sources, concerning density and position.

One diminishing fact is: the EBCM is not as easy to apply for simulating agglomerated particle scattering and grows extensively complicated when used to calculate scattering by particles, which enclose *large numbers* of inhomogeneities. In these cases the volume methods are more adequate.

REFERENCES

1. Wriedt, T., A review of elastic light scattering theories. *Part. Part. Syst. Charact.*, 1998, **15**, 67.
2. Flatau, P. J., Scattering by irregular particles in anomalous diffraction and discrete dipole approximations *Colorado State Univ., Dept. of Atmospheric Sci.*, 1992.
3. Flatau, P. J., Fuller, K. A. and Mackowski, D. W. Scattering by two spheres in contact: comparisons between discrete-dipole approximation and modal analysis, *Appl. Opt.*, 1992, **32**(18), 3302.
4. Hovenier, J. W., Lumme, K., Mishchenko, M. I., Voshchinnikov, N. V., Mackowski, D. W. and Rahola, J., Computations of scattering of four types of non-spherical particles using diverse methods, *JQSRT*, 1996, **55**(6), 695.
5. Cooper, J., Hombach, V. and Schiavoni, A., Comparison of computational electromagnetic codes applied to a sphere canonical problem, *IEEE Trans. Ant. Prop.*, 1996, **143**(4), 309.
6. Ku, J. C. and Shim, K.-H., A comparison of solutions for light scattering and absorption by agglomerated and arbitrarily shaped particles, *JQSRT*, 1992, **47**(3).
7. Lakhtakia, A. and Mulholland, G., On two numerical techniques for light scattering by dielectric agglomerated structures, *J. Res. Natl. Inst. Stand. Technol.*, 1993.
8. Purcel, E. M. and Pennypacker, C. R., Scattering and absorption of light by non-spherical dielectric grains, *Astrophys. J.*, 1973, **186**, 705–714.
9. Draine, B. T. and Goodman, J., Beyond Clausius-Mossotti: wave propagation on a polarizable point lattice and the discrete dipole approximation, *Astrophys. J.*, 1993, **405**, 685–697.
10. Goodman, J., Draine, B. T. and Flatau, P. J., Application of fast-Fourier-transform techniques to the discrete-dipole approximation, *Opt. Lett.*, 1991, **16**, 1198.
11. Peltoniemi, J., Electromagnetic scattering by irregular grains using variational volume integral equation method *JQSRT*, 1996.
12. Piller, N. B., Improved coupled dipole approximation for EM scattering, in Y. Eremin and T. Wriedt eds, *Electromagnetic and Light Scattering—Theory and Applications, Proc. Workshop 1997, Moscow*.
13. Flatau, P. J., Improvements in the discrete dipole approximation method of computing scattering and absorption, *Opt. Lett.*, 1997, **22**(16), 1205.
14. Kunz, K. S. and Luebbers R. J., *The Finite Difference Time Domain Method for Electromagnetics CRC Press*, Boca Raton, 1993.
15. Shang, J. S., Time-domain electromagnetic scattering simulations on multi-computers, *J. Comput. Phys.*, 1996, **128**, 381–390.
16. University of Brunel, U. K., Dept. of Elec. Eng. Parallel FDTD Project, www.brunel.ac.uk:8080/depts/fdtd/home.html.
17. Cole, J. B., High accuracy solution of Maxwell's equation using non-standard finite differences, *Comput. Phys.*, 1997, **11**(2).
18. Umashankar, K. and Taflove, A., A Novel Method to Analyse Electromagnetic Scattering of Complex Objects, *IEEE Trans. EMC*, 1982, EMC-24, 4.
19. Waterman, P. C., New formulation of acoustic scattering, *J. Acoust. Soc. Am.*, 1969, **45**, 1417.
20. Waterman, P. C., Symmetry, unitarity and geometry in electromagnetic scattering, *Phys. Rev. D*, 1971, **3**, 825–839.
21. Barber, P. W. and Hill, S. C., *Light Scattering by Particles: Computational Methods. World Scientific Singapore*, 1990.
22. Mishchenko, M. I., Travis, L. D. and Macke, A., Scattering of light by polydisperse randomly oriented finite circular cylinders *Appl. Opt.*, 1996, **35** (24), 4927.
23. Wriedt, T. and Doicu, A., Formulations of the extended boundary condition method for three-dimensional scattering using the method of discrete sources, *J. Modern Opt.*, accepted.